SvedbergOpen
DISSEMINATION OF KNOWLEDGE

International Journal of Artificial Intelligence and Machine Learning

Publisher's Home Page: https://www.svedbergopen.com/

Research Paper Open Access

Temperature Variation Effects on the Vibrational Behaviour of Trapezoidal Plate: An ANN – Based Prediction Technique

Urvashi Devi[a], Dr. Manoj Kumar Dhiman[b*]

[a]Doctoral student PhD, Department of Mathematics, Indus International University Bathu (Una), Himachal Pradesh, India.
[b] PhD, Associate Professor, Department of Mathematics, Indus International University Bathu (Una), Himachal Pradesh, India.
[*]Corresponding author: Dr. Manoj Kumar Dhiman, Email: m.manojdhiman@gmail.com

Abstract
This research scrutinized the effect of temperature variation on the vibrational analysis of a non – homogeneous trapezoidal – shaped plate with the consideration of dual – exponential thickness alteration. This examination evaluates a structural plate governed by C–C–C–S edge constraints, where three boundaries are rigidly supported and the remaining edge is supported in a simple manner. The study assesses the consequence of thermal variation on the primary two vibration-related modes. A governing vibrational formulation is constructed by applying Rayleigh–Ritz approach. Maple software is employed to measure frequency characteristics across various temperature scenarios. To complement the mathematical formulation, an Artificial Neural Network (ANN) model is constructed to predict the primary and secondary vibrational mode frequency values depending on the parameter of temperature variation. The numerical results acquired through the Rayleigh–Ritz scheme function as the baseline dataset for training, validation, and assessment the artificial neural network model.

Keywords: Trapezoidal – shaped plate, thermal – variation, vibrational behaviour, Rayleigh – Ritz strategy, frequency parameter, artificial neural network.

1. Introduction

The vibration behaviour of the plates has been scrutinized extensively as it plays an essential role to make designs and performance of numerous engineering structures. Plates function as primary load-bearing elements throughout diverse branches of engineering, comprising spacecraft, mechanical engineering, infrastructure, and shipbuilding. The system's dynamic properties is controlled by numerous factors, namely shape arrangement, substance properties, plate thickness allocation, edge conditions, and temperature are uniqueness. Amidst the numerous vibrational properties, eigenfrequencies and modal shapes are notably significant, because they reveal information about the inherent vibrational response of a structure as well as its sensitivity to outside disturbances.

For mathematical convenience, vibration assessment commonly presumes uniform-thickness plates. Nevertheless, this abstraction might not fully capture existing structures where properties of materials and thickness differ throughout the structure. These alterations immediately influence a plate's mechanical stiffness and mass arrangement, consequently altering the fundamental frequencies of vibration. The complexity level intensifies when behaviour of the material is directionally dependent, implying that its mechanical characteristics differ alongside primary structural orientations.

The spatial configuration of a plate considerably affects its vibrational properties. Whereas rectangular structures have been comprehensively examined, non-rectangular configurations are frequently encountered in real-world applications. To illustrate, trapezoid-shaped plates, distinguished by non-uniform dimensions in a particular direction, exhibit distinct vibrational responses when compared to their rectangular equivalents. Assessing vibrational behaviour in trapezoid-shaped plates gets increasingly problematic when integrated with directionally varying material attributes with non-constant thickness.

Additionally, plates are capable of operating experiencing diverse heat-related conditions, making necessary assessment regarding temperature distributions. Temperature differences have the ability to change material properties and produce temperature-induced stresses, consequently influencing eigenfrequencies and vibration modes. Prior investigations have indicated that temperature variations may impact vibrational behaviors of trapezoid-shaped plates possessing orthotropic properties, particularly when combined with uneven thickness and diverse material properties.

The vibration assessment of trapezoidal and additional irregularly shaped plates has been carried out utilizing different theoretical and computational techniques. As an illustration, the Rayleigh-Ritz approach has been employed to evaluate natural frequencies of trapezoid-shaped plates possessing orthotropic behaviour under diverse boundary and thermal environments. Existing literature has assessed the consequences of thickness fluctuations, thermal differences, and non-uniform material properties independently. Current research has emphasized directionally dependent trapezoidal plates exhibiting variations in thickness and compositional properties. Collectively, the conducted analyses demonstrate the considerable sensitivity of vibration characteristics to the combined effects arising from structural configuration, material features, thickness differences, and thermal environments.
Simultaneously with mathematical and numerical strategies, algorithmic approaches utilizing cutting-edge artificial intelligence approaches are gaining wider application in structural dynamics assessment. Artificial neural networks (ANNs), capable of uncovering correlations among input elements and system results, provide opportunities for assessing a comprehensive variety of vibration situations. In the context of this research, ANNs are designed to supplement, instead of replace, standard mathematical approaches, operating as a supplementary computational resource for the analysis of vibration modes. The chief purpose of the present investigation aims to describe the vibration characteristics of a precisely defined directionally dependent and non-uniformly shaped trapezoidal plate, considering the effects of thickness and temperature variations.

Özdilek, and others (2026) studied the natural vibrational-behavior of a functionally graded material plate by employing traditional mathematical strategies and machine learning strategies. They calculated the equations for finding the plate's natural frequencies and then built an ANN trained on exiting data to predict these frequencies in a very short time [1]. Eftekhari and others (2026) investigated a quick and efficient way to scrutinize the vibrational characteristics of the trapezoidal – thin plate. The material requires the time – consuming simulation with the consideration of changeability in shape, to overcome this issue, author created a reduced – order model to assess the plate's vibrational behavior without repeating the full-simulation [2]. Domagalski and others (2026) focused on machine-learning strategies to quickly forecast the vibrational – frequencies of thin rectangle – shaped plate with altering thickness. To speed the traditional approaches up, the author trained an ANN on data including different configurations of the plate, edge restrictions and thickness patterns [3].
Saini, R. (2025) discussed a review article focused on employing the new type of information processing tool to scrutinize the vibrational – response of beams, plates, shells etc., and also highlighted the implementations for assessing bending and vibrations [4]. Sharma, and others (2025) examined the vibrational behavior of an orthotropic trapezoidal – shaped plate with parabolically altering non – homogeneity and thermal-gradient. In this paper, the plate's thickness assumed to alter linear in one direction and parabolical in other with C-S-C-S (Clamped-simply supported-clamped-simply supported) edge restriction for the plate [5]. Suman, and others (2025) emphasizes the essentiality of free vibrational-approach and also introduces a novel combined strategy employing higher-order extended finite-element-method (HO-XFEM) along with the ANN-model to forecast the natural-frequencies of sandwich plates and generated 557 data points by HO-XFEM and then employed to trained the optimized ANN-model [6]. Ogbodo and others (2025) develops an ANN-model to predict the non-dimensional resonant frequencies of all-rounded clamped (C-C-C-C) thin rectangle – shaped plate with dynamic load. The model was trained and tested by employing 165 Rayleigh – Ritz generated datasets [7].
Van Delden, and others (2024) discussed that the deep-learning models can forecast the vibrations fastly but sometimes less accurately, so, on the contrast these techniques, author created a benchmark with 12000 distinct plate configurations, material and edge restrictions along with their vibrational data. They developed a new ANN-model that predicts the vibrational frequencies of the plate [8]. Prusty, and others (2024) discussed that polymers which are visco-elastic material exhibit the storage modulus and a loss factor that alter with frequency. The author introduces a NN-based (Neural Network – Based) method to assess these frequency-dependent features automatically leads to understand model visco-elastic material better [9]. Singh, D and others. (2024) studied that the configurational-discontinuities like cut-outs and material features like porosity significantly affects the Eigen-frequencies and mode-shapes. The author found that the H-OSDTs (higher-order shear deformation theories) are often employing for precise examination of thick-plates, and finite-element-method are popular but computationally-demanding, to overcome these challenges, an ANN-model strategies are rising employed to forecast the vibrational-responses efficiently [10].
Allah, M and others (2023) utilizes an ANN –model to predict the eigen-frequencies of the functionally-graded-material plate and ANN is trained by employing the datasets generated from a strategy called 3rd-order shear-deformation-theory and finite-element-strategy [11]. Taghizadeh and others (2023) explores the impleamentations of an ANN-model to predict the flexural deformation and flexural instability responses of dimension-dependent micro-sized plate made of 2-D functionally-graded materials. The author evolves an ANN-model with 9 and 10 input-factors for flexural deformation and flexural instability,

trained on large datasets of 8842 and 9980 random-data points and selected NN (neural network) architecture comprises 6-unobserved levels and 32-nodes each and got larger assessment coefficient [12]. Seba, and others (2022) develops a predictive-model to assess how the Eigen-frequencies of the plates made of numerous thin layers of different materials with eccentric cutouts varies their mechanical and configurational-features. The author combined their model with finite-element-method and ANN which is trained by the Levenberg-Marquardt algorithm [13]. Shenas, and others (2022) assessed the length-scale non-linear free vibrational behavior of FG (functionally graded) circumferential trapezoidal-shaped micro-sized plates with the consideration of 4-VRPT (4-variable refined plate theory) and MSGT (modified strained gradient theory). The author employed the Chebyshev's – Ritz strategy to formulate the non-linear governing equations and are assessed by repeated computations to evaluate non-linear frequencies during +ve and –ve deflections [14]. Heidari, and others (2022) introduces a novel approach to assess the free-vibrations of multiple-elastically connected rectangle-shaped plates. In this article, author considered the n-parallel plates that are connected elastically and also explores how the several features like plate's thickness, geometrical aspect ratio and constant of stiffness impacts the eigenfrequencies, and reveling that these effects alter significantly between low and high frequency modes based on the plate's edge restrictions [15].

Kallannavar, and others (2021) focuses on construct an anticipation-model to assess how the thermal profile and moisture affects the vibrational –behavior of skew laminated composite sandwich plate by employing ANN –model. Author also create a novel finite-element model which is based on 1st –order shear deformation theory, incorporating hygro-elastic and thermo-elastic consequences [16]. Saberi, and others (2021) present for the very 1st time employing the deep-learning strategy specifically ANN- model to scrutinize the free vibrational-analysis of the reactance-shaped dual-stable composite plates. Firstly, the author scrutinize the steady and time-dependent performance by analytical-approach namely FEM as well as empirical approach. The correlation demonstrates the fundamental discrepancies in the Eigen-frequencies with the analytical strategy precisely predict only the 4th-frequency ad failing to estimate 1st-three. To overcome this, a deep NN (neural network) is employed to model the model parameters enabling the estimation of Eigen-frequencies across stable configuration based on the plate's geometric dimensions [17].

Jamil, and others (2021) assess the implementations of NN (neural network) predictive controller as a novel framework for controlling vibrations in the tall-structures employing the single-degree of freedom active tuned mass damper (ATMD) [18]. Sinha, and others (2020) assessed both numerical and empirical scrutinization of woven-glass-fiber laminated composite stiffened-plate. A total 24-stiffenced plates, fabricated from the woven glass fiber and epoxy resin with hardener, were scrutinized in this investigation. Eigen-frequencies were assessed, and to validate the empirical outcomes, a model called FEM (finite element model) of the laminated composite plates was developed [19]. Zhang, and others (2020) emphasized the essential role of vibrational-analysis of the classic-elastic structures, especially the plate with the rectangular-configuration, for both vibration mitigation and ensuring reliable, secure and durable structural performance through optimal-design. The author assessed the impact on both free-vibrations and forced-vibrations with the alteration in edge-restrictions of the plate [20].

From a mathematical perspective, the approach is designed to discover eigenfrequencies including their corresponding modal shapes. Subsequently, the impact of framework and heat-related parameter T_v on vibrational performance is evaluated. An ancillary ANN-supported strategy is employed to support the evaluation of vibration characteristics extracted from the mathematical evaluation. Consequently, the present study emphasises the mathematical comprehension concerning the vibration features of the plate. The neural network element operates entirely as a complementary instrument for mode-specific analysis. This strategy retains standard vibration analysis fundamental to the effort while simultaneously exploring the potential of a straightforward algorithmic learning technique to assist in understanding the generated vibrational-modes.

2. Mathematical Modeling

2.1configuration and assumptions

Assess a trapezoidal – shaped configurational plate whose geometry is illustrated in the dimensionless coordinate system $(\delta,\ \varphi)$ as shown in fig. 1. The two vertical sides of the trapezoidal – shaped plate are detached with a distance 'a'. The heights of the left and right vertical sides are represented by 'b' and 'c', respectively.

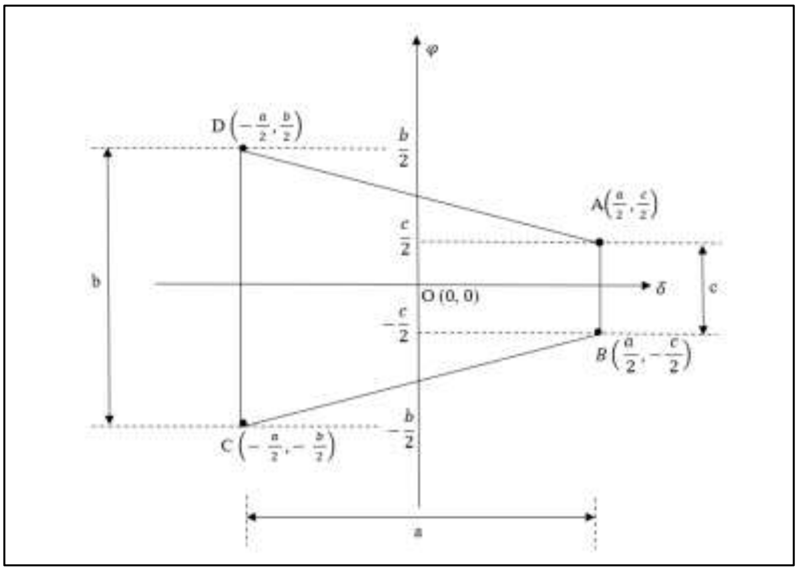

Fig. 1. Configuration of Trapezoidal – shaped plate

The four edges points of the trapezoidal – shaped plate are:
$A\left(\frac{a}{2},\frac{c}{2}\right)$, $B\left(\frac{a}{2},-\frac{c}{2}\right)$, $C\left(-\frac{a}{2},-\frac{b}{2}\right)$ and $D\left(-\frac{a}{2},\frac{b}{2}\right)$.
Thus, 'a' indicates the lateral distance among the two vertical sides that are parallel, while 'b' and 'c' indicates their corresponding elevations. The coordinates employed in the mathematical formulation are normalized as
$\delta = \frac{x}{a}, \varphi = \frac{y}{b}$
The trapezoidal – shaped plate's domain is consequently described by $-\frac{1}{2} \leq \delta \leq \frac{1}{2}$, while the upper and lower limits of the φ depend on δ. Form the geometry,
$\varphi_{upper} = \frac{c}{4b} - \frac{\delta}{2} + \frac{1}{4} + \frac{c\delta}{2b}$, and $\varphi_{lower} = -\frac{c}{4b} + \frac{\delta}{2} - \frac{1}{4} - \frac{c\delta}{2b}$.
Hence, the integration domain for the trapezoidal shaped plate is specified through these inclination boundary lines.

2.2Variable thickness of the trapezoidal – shaped plate

It is presumed that the plate possesses thickness that is variable across both coordinating orientations. The model implemented in the current assessment demonstrates the thickness through the application of a bi-exponential function,

$$d(\delta,\varphi) = d_0\left[\left(e^{1-\beta_1}\right)\left(\delta+\tfrac{1}{2}\right)\right]\left[\left(e^{1-\beta_2}\right)\left(\varphi+\tfrac{1}{2}\right)\right]$$

where β_1 *and* β_2 are the reduction constants associated with the two coordinate orientations, and d_0 = reference thickness of the trapezoidal plate obtained at
$\delta = -\frac{1}{2},\ \varphi = -\frac{1}{2}$.
To facilitate symbolical calculations, the exponential terms are approximated using Maclaurin series expansion of the exponential function and is expressed as
$e^p \approx 1 + \frac{p}{1!} + \frac{p^2}{2!} + \frac{p^3}{3!} + \frac{p^4}{4!} + \frac{p^5}{5!}$,
for the subsequent formulation, the exponential functions are stated by Taylor expansions truncated after the fifth – order term.
For p = $1-\beta_1$
$\therefore e^{(1-\beta_1)} \approx 1 + \frac{(1-\beta_1)}{1!} + \frac{(1-\beta_1)^2}{2!} + \frac{(1-\beta_1)^3}{3!} + \frac{(1-\beta_1)^4}{4!} + \frac{(1-\beta_1)^5}{5!}$
Similarly
For p = $1-\beta_2$
$\therefore e^{(1-\beta_2)} \approx 1 + \frac{(1-\beta_2)}{1!} + \frac{(1-\beta_2)^2}{2!} + \frac{(1-\beta_2)^3}{3!} + \frac{(1-\beta_2)^4}{4!} + \frac{(1-\beta_2)^5}{5!}$
Thus,

$$d(\delta) = d_0\left[\left(1 + \frac{(1-\beta_1)}{1!} + \frac{(1-\beta_1)^2}{2!} + \frac{(1-\beta_1)^3}{3!} + \frac{(1-\beta_1)^4}{4!} + \frac{(1-\beta_1)^5}{5!}\right)\left(\delta+\tfrac{1}{2}\right)\right]\left[\left(1 + \frac{(1-\beta_2)}{1!} + \frac{(1-\beta_2)^2}{2!} + \frac{(1-\beta_2)^3}{3!} + \frac{(1-\beta_2)^4}{4!} + \frac{(1-\beta_2)^5}{5!}\right)\left(\varphi+\tfrac{1}{2}\right)\right] \quad (1)$$

2.3Non – homogeneous material distribution

The mass density denoted by D of the trapezoidal – shaped plate is assumed to alter linearly along the δ – coordinate and corresponding variation in density is stated as:

$$D = D_0\left[1-(1-\alpha_1)\left(\delta+\frac{1}{2}\right)\right] \tag{2}$$

where D is varying mass density, D_0 represent the reference mass density and α_1 is the non – uniformity constant. At $\delta = -\frac{1}{2}$, the density attains its reference value i.e. D = D_0.

2.4 Distribution of temperature with bi – exponential alteration

The temperature distributed over the trapezoidal – shaped plate is assumed to alter in a bi – exponential manner and is expressed as:

$$t = t_0\left(e^{\frac{1}{2}}-e^{\delta}\right)\left(e^{\frac{1}{2}}-e^{\varphi}\right)$$

Where

't_0' = reference temperature and t = temperature distributed

Now again employing the Taylor – series expansion of the exponential terms up to fifth order as:

$$e^{\frac{1}{2}} \approx 1+\frac{\left(\frac{1}{2}\right)}{1!}+\frac{\left(\frac{1}{2}\right)^2}{2!}+\frac{\left(\frac{1}{2}\right)^3}{3!}+\frac{\left(\frac{1}{2}\right)^4}{4!}+\frac{\left(\frac{1}{2}\right)^5}{5!},$$

$$e^{\delta} \approx 1+\frac{\delta}{1!}+\frac{\delta^2}{2!}+\frac{\delta^3}{3!}+\frac{\delta^4}{4!}+\frac{\delta^5}{5!}$$

and

$$e^{\varphi} \approx 1+\frac{\varphi}{1!}+\frac{\varphi^2}{2!}+\frac{\varphi^3}{3!}+\frac{\varphi^4}{4!}+\frac{\varphi^5}{5!}$$

So, the expression becomes

$$t = t_0\left(1+\frac{\left(\frac{1}{2}\right)}{1!}+\frac{\left(\frac{1}{2}\right)^2}{2!}+\frac{\left(\frac{1}{2}\right)^3}{3!}+\frac{\left(\frac{1}{2}\right)^4}{4!}+\frac{\left(\frac{1}{2}\right)^5}{5!}-1-\frac{\delta}{1!}-\frac{\delta^2}{2!}-\frac{\delta^3}{3!}-\frac{\delta^4}{4!}-\frac{\delta^5}{5!}\right)\left(1+\frac{\left(\frac{1}{2}\right)}{1!}+\frac{\left(\frac{1}{2}\right)^2}{2!}+\frac{\left(\frac{1}{2}\right)^3}{3!}+\frac{\left(\frac{1}{2}\right)^4}{4!}+\frac{\left(\frac{1}{2}\right)^5}{5!}-1-\frac{\varphi}{1!}-\frac{\varphi^2}{2!}-\frac{\varphi^3}{3!}-\frac{\varphi^4}{4!}-\frac{\varphi^5}{5!}\right) \tag{3}$$

The young's modulus denoted by E^*, of the trapezoidal – shaped plate material is affected by the prescribed temperature modification. To incorporate this effect into the scrutinization, the temperature – dependent Young's modulus is stated as:

$$E^* = E_0\,(1-\gamma t) \tag{4}$$

where

E_0 = Young's modulus of plate material at the reference point,

γ = temperature coefficient demonstrating the variation of Young's modulus with temperature and

t = prescribed temperature change over the plate.

Now substituting eq^n. (3) in eq^n. (4), the expression becomes

$$E^* = E_0\left\{1-T_v\left(1+\frac{\left(\frac{1}{2}\right)}{1!}+\frac{\left(\frac{1}{2}\right)^2}{2!}+\frac{\left(\frac{1}{2}\right)^3}{3!}+\frac{\left(\frac{1}{2}\right)^4}{4!}+\frac{\left(\frac{1}{2}\right)^5}{5!}-1-\frac{\delta}{1!}-\frac{\delta^2}{2!}-\frac{\delta^3}{3!}-\frac{\delta^4}{4!}-\frac{\delta^5}{5!}\right)\left(1+\frac{\left(\frac{1}{2}\right)}{1!}+\frac{\left(\frac{1}{2}\right)^2}{2!}+\frac{\left(\frac{1}{2}\right)^3}{3!}+\frac{\left(\frac{1}{2}\right)^4}{4!}+\frac{\left(\frac{1}{2}\right)^5}{5!}-1-\frac{\varphi}{1!}-\frac{\varphi^2}{2!}-\frac{\varphi^3}{3!}-\frac{\varphi^4}{4!}-\frac{\varphi^5}{5!}\right)\right\} \tag{5}$$

For convenience, the combined temperature – variation parameter is introduced as $T_v = \gamma t_0$ and here, T_v represents the non – dimensional temperature – variation parameter, with $0 \le T_v \le 1$.

2.5 Non Strain energy ($E_{str.}$) and kinetic energy ($E_{kin.}$) formulation

For the vibrational analysis of the trapezoidal – shaped plate, the kinetic energy ($E_{kin.}$) and strain energy ($E_{str.}$) are expressed in terms of transverse displacement function as follows:

$$E_{kin.} = \frac{ab}{2}\,\omega^2\int d(\delta)D\omega^2\,dA \tag{6}$$

and the corresponding strain energy is given by

$$E_{str.} = \frac{ab}{2}\int B(\delta)\left[\left(\frac{1}{a^2}\frac{\partial^2\omega}{\partial\delta^2}+\frac{1}{b^2}\frac{\partial^2\omega}{\partial\varphi^2}\right)^2-2(1-R_p)\left[\left(\frac{1}{a^2b^2}\frac{\partial^2\omega}{\partial\delta^2}\frac{\partial^2\omega}{\partial\varphi^2}-\left(\frac{1}{ab}\frac{\partial^2\omega}{\partial\delta\,\partial\varphi}\right)^2\right)\right]\right]dA \tag{7}$$

where

R_p = Poisson proportional,

A = Expected area,

ω = Rotational frequency of the vibration of the plate and

$B\ (\delta)$ = Position – dependent bending stiffness coefficient associated with the plate formulation.

And bending stiffness $B(\delta)$ *is* expressed as:

$$B(\delta) = B_0\left\{\left[1-\left(1+\frac{(1-\beta_1)}{1!}+\frac{(1-\beta_1)^2}{2!}+\frac{(1-\beta_1)^3}{3!}+\frac{(1-\beta_1)^4}{4!}+\frac{(1-\beta_1)^5}{5!}\right)\left(\delta+\frac{1}{2}\right)\right]\left[1-\left(1+\frac{(1-\beta_2)}{1!}+\frac{(1-\beta_2)^2}{2!}+\frac{(1-\beta_2)^3}{3!}+\frac{(1-\beta_2)^4}{4!}+\frac{(1-\beta_2)^5}{5!}\right)\left(\varphi+\frac{1}{2}\right)\right]\right\}^3 \tag{8}$$

where

$\delta = \frac{x}{c}$ and $\varphi = \frac{y}{b}$ are the variables that are dimensionless.

$$B_0 = \frac{E^* {d_0}^3}{12(1 - {R_p}^2)} \tag{9}$$

Now using eq^n. (5) in eq^n. (9), the expression becomes

$$B_0 = \frac{E_0 \left\{ \begin{array}{l} 1 - T_v\left(1 + \frac{\left(\frac{1}{2}\right)}{1!} + \frac{\left(\frac{1}{2}\right)^2}{2!} + \frac{\left(\frac{1}{2}\right)^3}{3!} + \frac{\left(\frac{1}{2}\right)^4}{4!} + \frac{\left(\frac{1}{2}\right)^5}{5!} - 1 - \frac{\delta}{1!} - \frac{\delta^2}{2!} - \frac{\delta^3}{3!} - \frac{\delta^4}{4!} - \frac{\delta^5}{5!}\right) \\ \times \left(1 + \frac{\left(\frac{1}{2}\right)}{1!} + \frac{\left(\frac{1}{2}\right)^2}{2!} + \frac{\left(\frac{1}{2}\right)^3}{3!} + \frac{\left(\frac{1}{2}\right)^4}{4!} + \frac{\left(\frac{1}{2}\right)^5}{5!} - 1 - \frac{\varphi}{1!} - \frac{\varphi^2}{2!} - \frac{\varphi^3}{3!} - \frac{\varphi^4}{4!} - \frac{\varphi^5}{5!}\right) \end{array} \right\} {d_0}^3}{12(1 - {R_p}^2)}$$

$\therefore$ eq^n. (8) becomes,

$$B(\delta) = \frac{E_0 {d_0}^3}{12(1 - {R_p}^2)} \left\{ \begin{array}{l} 1 - T_v\left(1 + \frac{\left(\frac{1}{2}\right)}{1!} + \frac{\left(\frac{1}{2}\right)^2}{2!} + \frac{\left(\frac{1}{2}\right)^3}{3!} + \frac{\left(\frac{1}{2}\right)^4}{4!} + \frac{\left(\frac{1}{2}\right)^5}{5!} - 1 - \frac{\delta}{1!} - \frac{\delta^2}{2!} - \frac{\delta^3}{3!} - \frac{\delta^4}{4!} - \frac{\delta^5}{5!}\right) \\ \times \left(1 + \frac{\left(\frac{1}{2}\right)}{1!} + \frac{\left(\frac{1}{2}\right)^2}{2!} + \frac{\left(\frac{1}{2}\right)^3}{3!} + \frac{\left(\frac{1}{2}\right)^4}{4!} + \frac{\left(\frac{1}{2}\right)^5}{5!} - 1 - \frac{\varphi}{1!} - \frac{\varphi^2}{2!} - \frac{\varphi^3}{3!} - \frac{\varphi^4}{4!} - \frac{\varphi^5}{5!}\right) \end{array} \right\}$$
$$\times \left\{\left[1 - \left(1 + \frac{(1-\beta_1)}{1!} + \frac{(1-\beta_1)^2}{2!} + \frac{(1-\beta_1)^3}{3!} + \frac{(1-\beta_1)^4}{4!} + \frac{(1-\beta_1)^5}{5!}\right)\left(\delta + \frac{1}{2}\right)\right]\left[1 - \left(1 + \frac{(1-\beta_2)}{1!} + \frac{(1-\beta_2)^2}{2!} + \frac{(1-\beta_2)^3}{3!} + \frac{(1-\beta_2)^4}{4!} + \frac{(1-\beta_2)^5}{5!}\right)\left(\varphi + \frac{1}{2}\right)\right]\right\}^3 \tag{10}$$

Now employing eq^n. (1) and eq^n. (2) in eq^n. (6), the expression becomes

$$E_{kin.} = \frac{ab}{2} \omega^2 d_o D_o \int \left\{\left[\left(1 + \frac{(1-\beta_1)}{1!} + \frac{(1-\beta_1)^2}{2!} + \frac{(1-\beta_1)^3}{3!} + \frac{(1-\beta_1)^4}{4!} + \frac{(1-\beta_1)^5}{5!}\right)\left(\delta + \frac{1}{2}\right)\right]\left[\left(1 + \frac{(1-\beta_2)}{1!} + \frac{(1-\beta_2)^2}{2!} + \frac{(1-\beta_2)^3}{3!} + \frac{(1-\beta_2)^4}{4!} + \frac{(1-\beta_2)^5}{5!}\right)\left(\varphi + \frac{1}{2}\right)\right]\left[1 - (1-\alpha_1)\left(\delta + \frac{1}{2}\right)\right]\right\} \omega^2 dA \tag{11}$$

Now employing eq^n. (10) in eq^n. (7)

$$E_{str.} = \frac{ab \,.\, E_0 {d_0}^3}{24(1 - {R_p}^2)} \int \left\{ \left\{ \begin{array}{l} 1 - T_v\left(1 + \frac{\left(\frac{1}{2}\right)}{1!} + \frac{\left(\frac{1}{2}\right)^2}{2!} + \frac{\left(\frac{1}{2}\right)^3}{3!} + \frac{\left(\frac{1}{2}\right)^4}{4!} + \frac{\left(\frac{1}{2}\right)^5}{5!} - 1 - \frac{\delta}{1!} - \frac{\delta^2}{2!} - \frac{\delta^3}{3!} - \frac{\delta^4}{4!} - \frac{\delta^5}{5!}\right) \\ \times \left(1 + \frac{\left(\frac{1}{2}\right)}{1!} + \frac{\left(\frac{1}{2}\right)^2}{2!} + \frac{\left(\frac{1}{2}\right)^3}{3!} + \frac{\left(\frac{1}{2}\right)^4}{4!} + \frac{\left(\frac{1}{2}\right)^5}{5!} - 1 - \frac{\varphi}{1!} - \frac{\varphi^2}{2!} - \frac{\varphi^3}{3!} - \frac{\varphi^4}{4!} - \frac{\varphi^5}{5!}\right) \end{array} \right\} . \left\{\left[1 - \left(1 + \frac{(1-\beta_1)}{1!} + \frac{(1-\beta_1)^2}{2!} + \frac{(1-\beta_1)^3}{3!} + \frac{(1-\beta_1)^4}{4!} + \frac{(1-\beta_1)^5}{5!}\right)\left(\delta + \frac{1}{2}\right)\right]\left[1 - \left(1 + \frac{(1-\beta_2)}{1!} + \frac{(1-\beta_2)^2}{2!} + \frac{(1-\beta_2)^3}{3!} + \frac{(1-\beta_2)^4}{4!} + \frac{(1-\beta_2)^5}{5!}\right)\left(\varphi + \frac{1}{2}\right)\right]\right\}^3 \left[\left(\frac{1}{a^2}\frac{\partial^2 \omega}{\partial \delta^2} + \frac{1}{b^2}\frac{\partial^2 \omega}{\partial \varphi^2}\right)^2 - 2(1 - R_p)\left[\left(\frac{1}{a^2 b^2}\frac{\partial^2 \omega}{\partial \delta^2}\frac{\partial^2 \omega}{\partial \varphi^2} - \left(\frac{1}{ab}\frac{\partial^2 \omega}{\partial \delta \, \partial \varphi}\right)^2\right)\right]\right] \right\} dA \tag{12}$$

2.6Edge restrictions and assumed mode function

The plate is interpreted alongside the three clamping edges and one simply supported edge, designated by C – C – C – S configuration. The assumed displacement function must therefore satisfy the requirements associated with these four edge restrictions because the displacement function must meet the geometric requirements of the edge restrictions.

A two – term admissible function is adopted in the supplied formulation:

$$W = W_1 + W_2 = \left(\delta + \frac{1}{2}\right)^2 \left[\varphi - \left(\frac{b-c}{2}\right)\delta + \left(\frac{b+c}{4}\right)\right]^2 \left(\delta - \frac{1}{2}\right)^2 \left[\varphi + \left(\frac{b-c}{2}\right)\delta - \left(\frac{b+c}{4}\right)\right] . \left[\mathcal{E}_1 + \mathcal{E}_2\left(\delta + \frac{1}{2}\right)\left[\varphi - \left(\frac{b-c}{2}\right)\delta + \left(\frac{b+c}{4}\right)\right]\left(\delta - \frac{1}{2}\right)\left[\varphi + \left(\frac{b-c}{2}\right)\delta - \left(\frac{b+c}{4}\right)\right]\right] \tag{13}$$

where $\mathcal{E}_1$ and $\mathcal{E}_2$ are supposed to be unknown coefficients.

The acceptable function is chosen so that the needed movement limits are met along the edges that are fixed and the edges that are supported. The two unknown values are then found using the Rayleigh – Ritz strategy.

2.7 Rayleigh – Ritz formulation

The Ritz-Rayleigh method determines normal mode frequencies by finding where the difference between strain and kinetic energy ceases to change.

Thus,

$\zeta(E_{str.} - E_{kin.}) = 0$

After substituting the admissible displacement function and the limits of integration that describe the trapezoidal–shaped plate domain, the energy expressions become functions of the unknown coefficients $\mathcal{E}_1$ and $\mathcal{E}_2$.
We can also show the characteristic equation using a matrix format as

$$[S - \omega^2 M]h = 0,$$

where S is the stiffness matrix, M is the mass matrix and h = $\begin{bmatrix}\mathcal{E}_1\\ \mathcal{E}_2\end{bmatrix}$.
For a non – trivial solution,
det $[S - \omega^2 M] = 0$, solving the characteristic equation reveals the specific frequencies that the trapezoidal plate can naturally vibrate at. The associated eigenvectors indicate the relative influence of each section in shaping the plate's unique vibrational patterns.

2.8 Frequency parameters assessed from the Rayleigh – Ritz strategy

The resulting equation provides the frequency parameters corresponding to the first two vibrational modes of the trapezoidal plate. In the present analysis, Maple software is employed to solve the characteristic equation and obtain the natural frequencies corresponding to the first two vibrational modes of the trapezoidal plate.

Table.1. (i)

Table 1. states the relationship among the frequency parameter (λ) and heat flow gradient (T_v). We have seen that, as the heat flow gradient rises from 0.0 to 1.0, the frequencies for both the modes diminishes as we go through the table from left to right for the following two parameters non – uniformity constant and reduction constants:
(i) $\alpha_1 = 0, \beta_1 = 0, \beta_2 = 0.2$
(ii) $\alpha_1 = 0, \beta_1 = 0.2, \beta_2 = 0.4$
(iii) $\alpha_1 = 0, \beta_1 = 0.4, \beta_2 = 0.6$
In other words, a higher heat flow gradient can lower the vibrational frequencies.

Frequency parameter (λ) vs. heat flow gradient (T_v)

T_v	$\frac{a}{b}$=1.0, $\frac{c}{b}$=1.0					
	$\alpha_1 = 0$					
	$\beta_1 = 0, \beta_2 = 0.2$		$\beta_1 = 0.2, \beta_2 = 0.4$		$\beta_1 = 0.4, \beta_2 = 0.6$	
	λ_1	λ_2	λ_1	λ_2	λ_1	λ_2
0.0	46.61709384	282.2348344	24.51894938	148.4445739	10.42711257	63.26547788
0.2	46.07891921	280.8246306	24.23589533	147.7028616	10.30545256	62.94953159
0.4	45.53346979	279.4074585	23.94900899	146.9574832	10.18213989	62.63203487
0.6	44.98045314	277.9832159	23.65814335	146.2083862	10.05692865	62.31293639
0.8	44.41955820	276.5517983	23.36313926	145.4555162	9.930071143	61.99226570
1.0	43.85045173	275.1130985	23.06381950	144.6988165	9.801212959	61.66995456

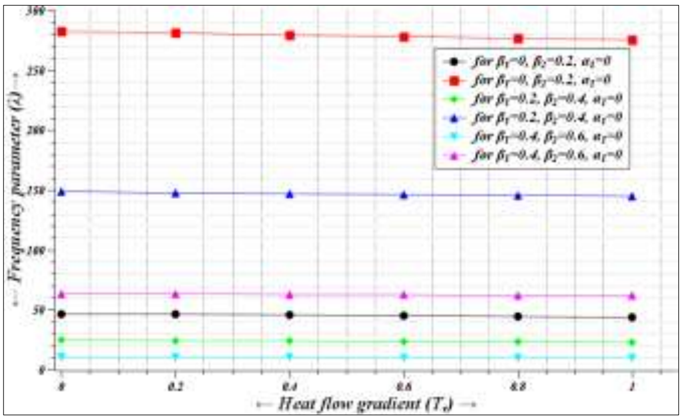

Fig. 2. Frequency parameter (λ) vs. heat flow gradient (T_v)

Table.2. (ii)

Table 2. (ii) displays the connection among the frequency parameter (λ) and Heat flow gradient (T_v)and as we go through the table from left to right the Heat flow gradient rises from 0.0 to 1.0 which results the

frequencies for both the modes diminishes for the different values of two parameters non – uniformity constant and reduction constants:
(i) $\alpha_1 = 0.2$, $\beta_1 = 0, \beta_2 = 0.2$
(ii) $\alpha_1 = 0.2$, $\beta_1 = 0.2$, $\beta_2 = 0.4$
(iii) $\alpha_1 = 0.2$, $\beta_1 = 0.4, \beta_2 = 0.6$

Frequency parameter (λ) vs. Heat flow gradient (T_v)

T_v	$\frac{a}{b}=1.0, \frac{c}{b}=1.0$					
	$\alpha_1 = 0.2$					
	$\beta_1 = 0, \beta_2 = 0.2$		$\beta_1 = 0.2, \beta_2 = 0.4$		$\beta_1 = 0.4, \beta_2 = 0.6$	
	λ_1	λ_2	λ_1	λ_2	λ_1	λ_2
0.0	41.96169439	251.4061456	22.07031150	132.2298897	9.356052062	56.35998312
0.2	41.47781165	250.1466781	21.81580643	131.5674585	9.246087364	56.07785115
0.4	40.98737881	248.8809754	21.55785864	130.9017483	9.134772647	55.79435622
0.6	40.49013017	247.6089458	21.29632461	130.2327101	9.021671276	55.50941662
0.8	39.98578640	246.3304958	21.03106173	129.5602955	8.906987900	55.22305607
1.0	39.47404699	245.0455292	20.76190497	128.8844528	8.790509055	54.93523034

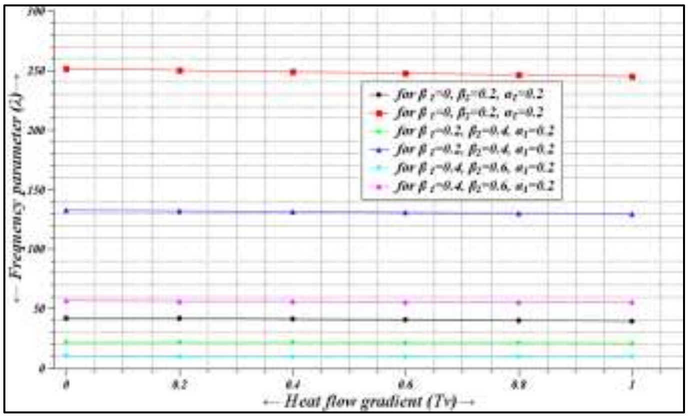

Fig. 3. Frequency parameter (λ) vs. heat flow gradient (T_v)

Table.2.

Table 2 indicates the relationship between the frequency parameters of the first and second modes and the reduction constants. While examining the table from left to right, we scrutinized that as the value of reduction constants escalates from 0.0 to 1.0, both the modes of vibrations rise for the various values of other parameters like heat flow gradient and non–uniformity constants as:
(i) $\alpha_1 = 0.1, T_v = 0$
(ii) $\alpha_1 = 0.3, T_v = 0.4$
(iii) $\alpha_1 = 0.5, T_v = 0.8$

Frequency parameter (λ) vs. reduction constants (β_1, β_2)

$\beta_1 = \beta_2$	$\frac{a}{b}=1.0, \frac{c}{b}=0.5$					
	$\alpha_1 = 0.1$		$\alpha_1 = 0.3$		$\alpha_1 = 0.5$	
	$T_v = 0$		$T_v = 0.4$		$T_v = 0.8$	
	λ_1	λ_2	λ_1	λ_2	λ_1	λ_2
0.0	62.95174237	378.9081147	55.90856269	338.2135064	50.35499140	307.2769341
0.1	48.58664454	292.4442304	43.15066358	261.0358152	38.86437402	237.1587281
0.2	36.57472075	220.1441333	32.48266041	196.5007253	29.25605562	178.5266977
0.3	26.67789075	160.5746116	23.69310248	143.3289519	21.33959149	130.2185761
0.4	18.67380166	112.3979435	16.58437862	100.3264679	14.93693726	91.14956283
0.5	12.33722266	74.37713814	10.95371571	66.38953723	9.864810119	60.31695453

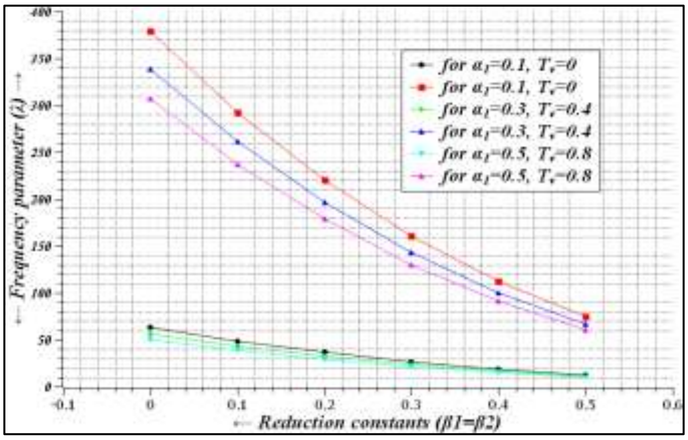

Fig. 4. Frequency parameter (λ) vs. reduction constants (β_1, β_2)

Table. 3.

The connection among the non–uniformity constants and frequency parameter for the first and second mode is observed. During the approach of analyzing the configuration of the table from left to right, we have perceived, both modes of vibration pitch down for the various values of other parameters like heat flow gradient and reduction constants whenever the value of non–uniformity constants enhances from 0.0 to 1.0.

(i) $\beta_1 = 0$, $\beta_2 = 0.2$, $T_v = 0$

(ii) $\beta_1 = 0.2$, $\beta_2 = 0.4$, $T_v = 0.2$

(iii) $\beta_1 = 0.4$, $\beta_2 = 0.6$, $T_v = 0.4$

Frequency parameter (λ) vs. Non – uniformity constant (α_1)

α_1	$\frac{a}{b}=1.0, \frac{c}{b}=1.0$					
	$T_v = 0$, $\beta_1 = 0$, $\beta_2 = 0.2$		$T_v = 0.2$ $\beta_1 = 0.2$, $\beta_2 = 0.4$		$T_v = 0.4$ $\beta_1 = 0.4$, $\beta_2 = 0.6$	
	λ_1	λ_2	λ_1	λ_2	λ_1	λ_2
0.0	46.61709384	282.2348344	24.23589533	147.7028616	10.18213989	62.63203487
0.2	41.96169439	251.4061456	21.81580643	131.5674585	9.134772647	55.79435622
0.4	38.46996148	228.9216957	20.00061906	119.7996719	8.366498027	50.80490051
0.6	35.72606064	211.5790610	18.57417067	110.7231657	7.769415249	46.95556831
0.8	33.49627579	197.6719821	17.41497953	103.4448189	7.286726767	43.86841528
1.0	31.63782535	186.1957424	16.44881925	97.43873819	6.885665444	41.32076286

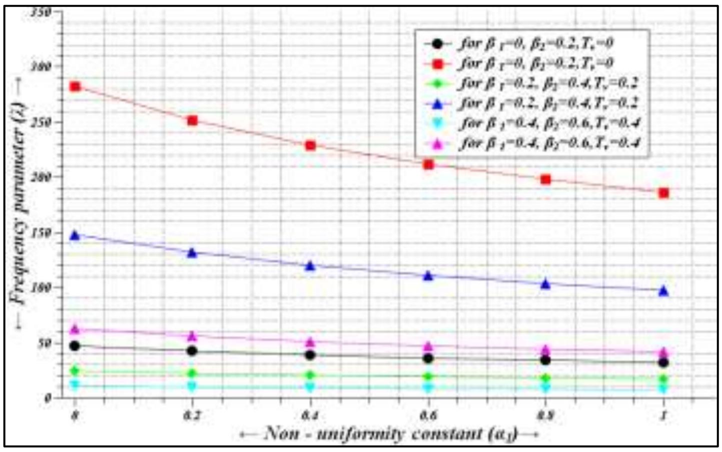

Fig. 5. Frequency parameter (λ) vs. Non–uniformity constant (α_1)

3. ANN–based analysis of the frequency modes

3.1 Objective of the ANN analysis

The analytical formulation described previously generates the primary as well as secondary frequency modes related to a trapezoidal plate through various permutations of configurational, thermal condition,

thickness-related, and constituent properties. Considering the correlation of frequency properties with numerous simultaneous factors, an Artificial Neural Network (ANN) is employed as an auxiliary computational instrument.
The intent of this neural network architecture is designed to forecast the initial two vibration frequency factors. Consequently, the ANN model is not intended to displace the Rayleigh-Ritz technique or the Maple-based numerical method. Alternatively, its objective is to verify whether a simple data-driven model can precisely reproduce the frequency variables extracted from the existing numerical formulation. Input features used in the ANN are directly extracted from the quantities employed in the computational investigation, and the corresponding frequency parameters obtained via the Rayleigh-Ritz technique serve as the expected outputs.

3.2Input and output parameters

Six parameters are considered as the inputs to the ANN model:
X = $\left\{\beta_1,\ \beta_2\ ,\ \frac{a}{b}\ ,\frac{c}{b}, T_v, \alpha_1\right\}$, here β_1, and $represent$ the thickness – reduction parameters, $\frac{a}{b}$ and $\frac{c}{b}$ describe the plate's geometry, T_v represents the thermal – parameter and α_1 describe the non – uniformity constant.
The corresponding output vector contains the first two frequency patterns as:
Y = $\{\lambda_1,\ \lambda_2\}$.
Thus, ANN establishes the following mapping:
$\left\{\beta_1,\ \beta_2\ ,\ \frac{a}{b}\ ,\frac{c}{b}, T_v, \alpha_1\right\} \rightarrow \{\lambda_1,\ \lambda_2\}$,
In this configuration, both vibrational modes can be determined simultaneously from the same initial parameters.

3.3Generation of the ANN – Dataset

The ANN dataset originates from a simulation model, as opposed to measurements we hypothesised during experiments. We have supplied distinct configurations involving six input quantities within the Rayleigh–Ritz procedure. Subsequently, we computed the respective values of λ_1 and λ_2 by using Maple.
Therefore, each numeric instance comprises a total of seven data points: the set of six model inputs and both frequency measurements. The essential arrangement of the dataset provided is illustrated in the table below:
Table. 4.

Case	β_1	β_2	$\frac{a}{b}$	$\frac{c}{b}$	T_v	α_1	λ_1	λ_2
1	0.0	0.2	1.0	1.0	0.0	0.0	46.61709384	282.2348344
2	0.0	0.2	1.0	1.0	0.2	0.0	46.07891921	280.8246306
3	0.0	0.2	1.0	1.0	0.4	0.0	45.53346979	279.4074585
4	0.0	0.2	1.0	1.0	0.6	0.0	44.98045314	277.9832159
5	0.0	0.2	1.0	1.0	0.8	0.0	44.41955820	276.5517983
6	0.0	0.2	1.0	1.0	1.0	0.0	43.85045173	275.1130985
7	0.2	0.4	1.0	1.0	0.0	0.0	24.51894938	148.4445739
8	0.2	0.4	1.0	1.0	0.2	0.0	24.23589533	147.7028616
9	0.2	0.4	1.0	1.0	0.4	0.0	23.94900899	146.9574832
10	0.2	0.4	1.0	1.0	0.6	0.0	23.65814335	146.2083862
11	0.2	0.4	1.0	1.0	0.8	0.0	23.36313926	145.4555162
12	0.2	0.4	1.0	1.0	1.0	0.0	23.06381950	144.6988165
13	0.4	0.6	1.0	1.0	0.0	0.0	10.42711257	63.26547788
14	0.4	0.6	1.0	1.0	0.2	0.0	10.30545256	62.94953159
15	0.4	0.6	1.0	1.0	0.4	0.0	10.18213989	62.63203487
16	0.4	0.6	1.0	1.0	0.6	0.0	10.05692865	62.31293639
17	0.4	0.6	1.0	1.0	0.8	0.0	9.930071143	61.99226570
18	0.4	0.6	1.0	1.0	1.0	0.0	9.801212959	61.66995456
19	0.0	0.2	1.0	1.0	0.0	0.2	41.96169439	251.4061456
20	0.0	0.2	1.0	1.0	0.2	0.2	41.47781165	250.1466781
21	0.0	0.2	1.0	1.0	0.4	0.2	40.98737881	248.8809754
22	0.0	0.2	1.0	1.0	0.6	0.2	40.49013017	247.6089458
23	0.0	0.2	1.0	1.0	0.8	0.2	39.98578640	246.3304958
24	0.0	0.2	1.0	1.0	1.0	0.2	39.47404699	245.0455292
25	0.2	0.4	1.0	1.0	0.0	0.2	22.07031150	132.2298897

26	0.2	0.4	1.0	1.0	0.2	0.2	21.81580643	131.5674585
27	0.2	0.4	1.0	1.0	0.4	0.2	21.55785864	130.9017483
28	0.2	0.4	1.0	1.0	0.6	0.2	21.29632461	130.2327101
29	0.2	0.4	1.0	1.0	0.8	0.2	21.03106173	129.5602955
30	0.2	0.4	1.0	1.0	1.0	0.2	20.76190497	128.8844528
31	0.4	0.6	1.0	1.0	0.0	0.2	9.356052062	56.35998312
32	0.4	0.6	1.0	1.0	0.2	0.2	9.246087364	56.07785115
33	0.4	0.6	1.0	1.0	0.4	0.2	9.134772647	55.79435622
34	0.4	0.6	1.0	1.0	0.6	0.2	9.021671276	55.50941662
35	0.4	0.6	1.0	1.0	0.8	0.2	8.906987900	55.22305607
36	0.4	0.6	1.0	1.0	1.0	0.2	8.790509055	54.93523034

4. Artificial Neural Network – Based Verification

To assess the effectiveness of a data-driven approach for predicting the vibrational behaviour of the trapezoidal plate structure, a simple artificial neural network (ANN) was constructed. This network was optimised using frequency measurements generated by the Rayleigh-Ritz variational formulation.
A feed-forward neural network was employed, incorporating a single hidden neural layer having 20 hidden units. The hidden layer implemented a rectified linear unit (ReLU) activation, while the network output layer employed a linear output activation. The model's input and output data were processed while data normalization before model training to ensure stable numerical behavior. Model training of the Artificial Neural Network (ANN) was executed employing the Adam optimization technique, with the Mean Squared Error (MSE) functioning as the training loss function.

The model was optimized on the set of 36 cases summarized in Table 4, computed from the Rayleigh-Ritz variational formulation. We then converted the ANN-predicted values back to their initial frequency-parameter representation and evaluated them against the relevant Rayleigh–Ritz predictions. Maximal absolute percentage deviations were measured to be **0.4111% for λ_1 and 0.5422% for λ_2**. The observed comparatively limited deviations demonstrate strong correspondence between the ANN-based predictions and the Rayleigh–Ritz predictions.

Consequently, the artificial neural network (ANN) model supplies an uncomplicated computational technique for predicting the initial two frequency-related parameters within the range of input variables investigated. Within this framework, the artificial neural network (ANN) model operates as a **supplementary verification tool**, with the Rayleigh-Ritz formulation method remaining the main approach for characterizing vibrational characteristics.

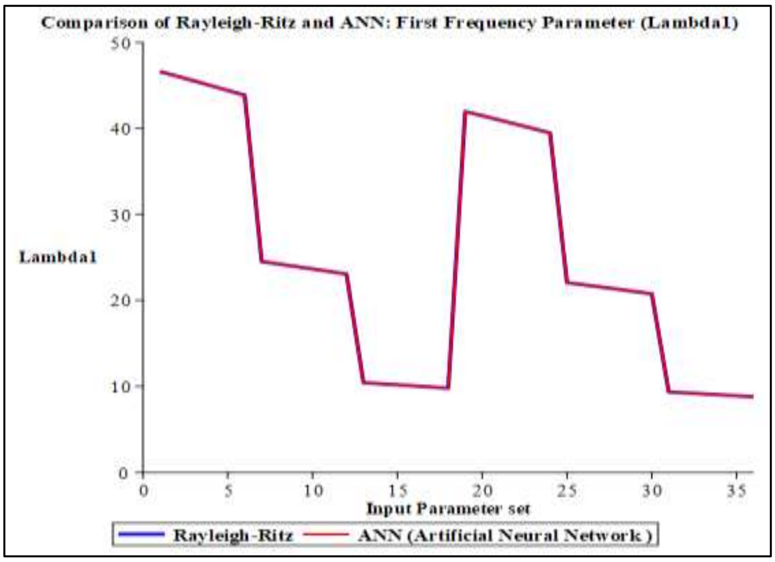

Fig. 6. Comparison of Rayleigh – Ritz and ANN predictions for the first frequency parameter

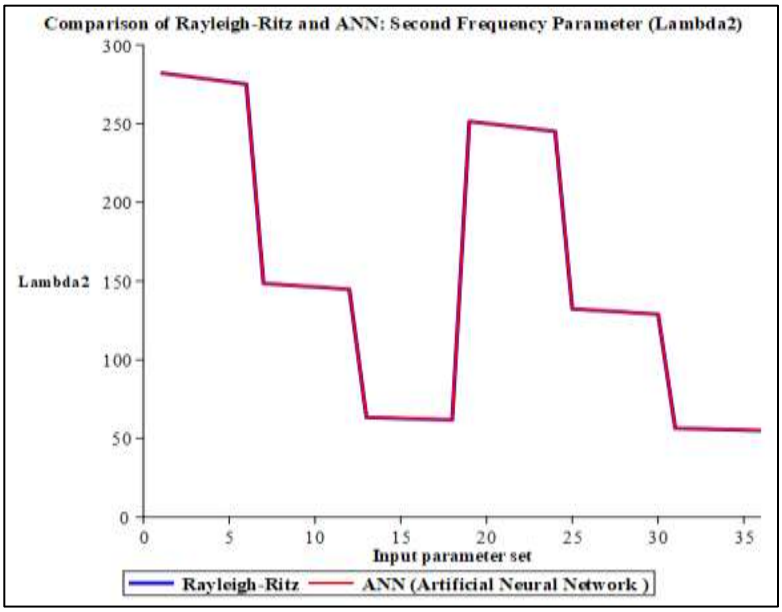

Fig. 7. Comparison of Rayleigh – Ritz and ANN predictions for the second frequency parameter

Figure 6 and Figure 7 demonstrate a comparative analysis among the Rayleigh-Ritz and Artificial Neural Network (ANN) results concerning the initial and second frequency parameters (λ_1 and λ_2, correspondingly). The data curves extracted from the dual approaches demonstrate substantial similarity through the entirety of reviewed conditions. More precisely, the greatest relative variation regarding the initial frequency parameter was determined to be approximately 0.4111%, and considering the second frequency parameter, it was 0.5422%. This strong correlation demonstrates that the artificial neural network is capable of accurately reproducing the changes in frequency parameters predicted by the Rayleigh-Ritz formulation. The observations additionally demonstrate that the artificial neural network might function as a functional simulation tool for approximating the vibrational behavior of plates within the investigated range of parameters in the current study.

5. Discussion of results

The numerical results generated from the Rayleigh – Ritz formulation demonstrate the clear alteration in the frequency parameters with the consideration of variations in the selected plate parameters. The initial two frequency parameters λ_1 and λ_2 were assessed for 36 combinations of the input parameters and generated outcomes were subsequently employed for the ANN – based computational verification. For the first frequency parameter λ_1, the assessed values demonstrate a decreasing tendency as the heat flow gradient T_v rises for a fixed combination of the remaining parameters. For instance, when β_1=0, $\beta_2 = 0.2, \frac{a}{b} = 1, \frac{c}{b} = 1$ and $\alpha_1 = 0$, the value of λ_1 diminishes from approximately 46.61709384 to 43.85045173 as T_v varies from 0 to 1. A similar reduction is observed for the other combinations of parameters.

The same general behavior is also observed for the second frequency parameter λ_2, for the above combination of parameters, its value diminishes approximately from 282.2348344 to 275.1130985 over the same range of T_v. consequently, the enhancement in the heat flow gradient produces a reduction in both the frequency parameters within the range considered in the present scrutiny.

The maximum relative deviation originated from the present scrutinization are approximately 0.411% and 0.542% for first and second modes of vibrations and these deviations are small as compared with the magnitude of the corresponding frequency parameters.

6. Conclusion

The present study highlights the influence of the considered parameters on the vibration behavior of the plate. The first two frequency parameters obtained using the Rayleigh–Ritz method show consistent changes with the variation of the selected parameters. The ANN results were found to be in close agreement with the Rayleigh–Ritz values for the 36 cases considered. Thus, the ANN provides a simple and useful additional check of the calculated frequency parameters without replacing the main Rayleigh–Ritz formulation.

7. References

[1]. Özdilek, E. E., Gündoğdu, E., Çelik, M., & Demirkan, E. (2026). Vibration Analysis of FGM Plate: A Hybrid Analytical and Machine Learning Approach. In *Nonlinear Dynamical Control, Computer Simulation and Optimization Systems: Theory and Applications* (pp. 275-285),

https://doi.org/10.1142/9789819815432_0025.
[2]. Eftekhari, S. A., Lee, K. H., & Lim, H. J. (2026). A unified physics-based framework for vibration prediction and design optimization of functionally graded trapezoidal thin plates. *Composite Structures*, 120841, https://doi.org/10.1016/j.compstruct.2026.120841.
[3]. Domagalski, Ł., & Kowalczyk, I. (2026). Application of Machine Learning Models in Predicting Vibration Frequencies of Thin Variable Thickness Plates. *Materials*, *19*(1), 205, https://doi.org/10.3390/ma19010205.
[4]. Saini, R. (2025). A review on artificial neural networks for structural analysis. *Journal of Vibration Engineering & Technologies*, *13*(2), 142, https://doi.org/10.1007/s42417-024-01749-7.
[5]. Sharma, A., & Sharma, P. (2025). Effect of Parabolically Varying Non-Homogeneity on Thermally Induced Vibration of Orthotropic Trapezoidal Plate with Thickness Varies Linearly in One Direction and Parabolically in Other Direction. *Engineering Mathematics*, *9*(1), 16-25, https://doi.org/10.11648/j.engmath.20250901.12.
[6]. Suman, S., Dwivedi, K., Raza, A., & Pathak, H. (2025). Accelerating composite sandwich plate analysis: A hybrid higher-order XFEM and ANN approach for natural frequency prediction. *Mechanics Based Design of Structures and Machines*, *53*(6), 4711-4723, https://doi.org/10.1080/15397734.2025.2454351.
[7]. Ogbodo, M., Onwuka, D. O., Okere, C. E., & Onwuka, U. S. (2025). Dynamic analysis of isotropic All Round Clamped (CCCC) Thin rectangular plate using Artificial Neural Network. *Journal of Materials Engineering, Structures and Computation*, *4*(2), https://doi.org/10.5281/zenodo.15535217.
[8]. Van Delden, J., Schultz, J., Blech, C., Langer, S. C., & Lüddecke, T. (2024). Learning to predict structural vibrations. *Advances in Neural Information Processing Systems*, *37*, 103706-103736, https://doi.org/10.52202/079017-3294.
[9]. Prusty, J. K., Papazafeiropoulos, G., & Mohanty, S. C. (2024). Experimental verification of the neural network optimization algorithm for identifying frequency-dependent constitutive parameters of viscoelastic materials. *Journal of Vibration Engineering & Technologies*, *12*(2), 2147-2173, https://doi.org/10.1007/s42417-023-00972-y.
[10]. Singh, D., Rai, S., & Gupta, A. (2024). Vibration analysis of sandwich functionally graded material plate with cut-outs using artificial neural network technique. *Thin-Walled Structures*, *202*, 112072, https://doi.org/10.1016/j.tws.2024.112072.
[11]. Allah, M. J., Hassouna, S., Aitbelale, R., & Timesli, A. (2023). Free vibration analysis of FGM plates using an optimization methodology combining artificial neural networks and third order shear deformation theory. *Steel & Composite structures: an international journal*, *49*(6), 633-643, https://dx.doi.org/10.12989/scs.2023.49.6.633.
[12]. Taghizadeh, M., Mahdavian, M., & Askari, A. R. (2023). Size-dependent bending and buckling of two-dimensional functionally graded microplates, an artificial neural network approach. *Physica Scripta*, *98*(10), 106001, https://doi.org/10.1088/1402-4896/acf2cd.
[13]. Seba, M. R., & Kebdani, S. (2022). Finite element and neural network based predictive model to determine natural frequency of laminated composite plates with eccentric cutouts under free vibration. *Advances in Technology Innovation*, *7*(2), 131, https://doi.org/10.46604/aiti.2022.8909.
[14]. Shenas, A. G., Ziaee, S., & Malekzadeh, P. (2022). Nonlinear free vibration of rotating FG trapezoidal microplates in thermal environment. *Thin-Walled Structures*, *170*, 108614, https://doi.org/10.1016/j.tws.2021.108614.
[15]. Heidari, E., & Ariaei, A. (2022). A new approach for free vibration analysis of a system of elastically interconnected similar rectangular plates. *Earthquake Engineering and Engineering Vibration*, *21*(4), 947-967, https://doi.org/10.1007/s11803-022-2129-9.
[16]. Kallannavar, V., Kattimani, S., Soudagar, M. E. M., Mujtaba, M. A., Alshahrani, S., & Imran, M. (2021). Neural network-based prediction model to investigate the influence of temperature and moisture on vibration characteristics of skew laminated composite sandwich plates. *Materials*, *14*(12), 3170, https://doi.org/10.3390/ma14123170.
[17]. Saberi, S., Ghayour, M., Mirdamadi, H. R., & Ghamami, M. (2021). Free vibration analysis and mode management of bistable composite laminates using deep learning. *Archive of Applied Mechanics*, *91*(6), 2795-2816, https://doi.org/10.1007/s00419-021-01930-4.
[18]. Jamil, M., Khan, M. N., Rind, S. J., Awais, Q., & Uzair, M. (2021). Neural network predictive control of vibrations in tall structure: An experimental controlled vision. *Computers & Electrical Engineering*, *89*, 106940, https://doi.org/10.1016/j.compeleceng.2020.106940.
[19]. Sinha, L., Mishra, S. S., Nayak, A. N., & Sahu, S. K. (2020). Free vibration characteristics of laminated composite stiffened plates: Experimental and numerical investigation. *Composite Structures*, *233*, 111557, https://doi.org/10.1016/j.compstruct.2019.111557.
[20]. Zhang, Y., & Du, J. (2020). Influence of boundary conditions on three-dimensional vibration characteristics of thick rectangular plates. *Science Progress*, *103*(4), 0036850420969548, https://doi.org/10.1177/0036850420969548.